Anal Bioanal Chem
DOI 10.1007/s00216-014-8282-x

RESEARCH PAPER

Direct and mediated electrochemistry of peroxidase and its electrocatalysis on a variety of screen-printed carbon electrodes: amperometric hydrogen peroxide and phenols biosensor

Fereshteh Chekin · Lo Gorton · Issa Tapsobea

Received: 29 April 2014 / Revised: 12 October 2014 / Accepted: 17 October 2014

Abstract This study compares the behaviour of direct and mediated electrochemistry of horseradish peroxidase (HRP) immobilised on screen-printed carbon electrodes (SPCEs), screen-printed carbon electrodes modified with carboxyl-functionalised multi-wall carbon nanotubes (MWCNT-SPCEs) and screen-printed carbon electrodes modified with carboxyl-functionalised single-wall carbon nanotubes (SWCNT-SPCEs). The techniques of cyclic voltammetry and amperometry in the flow mode were used to characterise the properties of the HRP immobilised on screen-printed electrodes. From measurements of the mediated and mediatorless currents of hydrogen peroxide reduction at the HRP-modified electrodes, it was concluded that the fraction of enzyme molecules in direct electron transfer (DET) contact with the electrode varies substantially for the different electrodes. It was observed that the screen-printed carbon electrodes modified with carbon nanotubes (MWCNT-SPCEs and SWCNT-SPCEs) demonstrated a substantially higher percentage (≈100 %) of HRP molecules in DET contact than the screen-printed carbon electrodes (≈60 %). The HRP-modified electrodes were used for determination of hydrogen peroxide in mediatorless mode. The SWCNT-SPCE gave the lowest detection limit (0.40±0.09 μM) followed by MWCNT-SPCE (0.48±0.07 μM) and SPCE (0.98±0.2 μM). These modified electrodes were additionally developed for amperometric determination of phenolic compounds. It was found that the SWCNT-SPCE gave a detection limit for catechol of 110.2±3.6 nM, dopamine of 640.2±9.2 nM, octopamine of 3341±15 nM, pyrogallol of 50.10±2.9 nM and 3,4-dihydroxy-L-phenylalanine of 980.7±8.7 nM using 50 μM H_2O_2 in the flow carrier.

Keywords Screen-printed carbon electrodes · Peroxidase · Hydrogen peroxide · Phenolic compounds

F. Chekin (✉)
Department of Chemistry, Ayatollah Amoli Branch, Islamic Azad University, 46178-678 Amol, Iran
e-mail: fchekin@yahoo.com

L. Gorton
Department of Analytical Chemistry, University of Lund, Box 124, 221 00 Lund, Sweden

I. Tapsobea
Laboratoire de Chimie Organique: Structure et Réactivité. UFR/SEA, Département de Chimie, Université de Ouagadougou, 03 BP 7021, Ouagadougou 03, Burkina Faso

Introduction

Peroxidases are important enzymes in bioanalytical chemistry. They are widely used for the construction of biosensors and are commonly used as enzyme labels in immunoassays [1–3]. Depending on the practical needs, different redox enzymes have been used in biosensor design, e.g. various specific and non-specific oxidases, dehydrogenases, peroxidases, etc. [4]. Horseradish peroxidase (HRP) with a molar weight of about 42 kDa and a diameter of about 5 nm is a glycosylated redox enzyme, which contains a heme prosthetic group as cofactor in its active site [5].

HRP-modified electrodes can be used for amperometric detection of the oxidative substrates of the enzyme (hydrogen peroxide, organic hydroperoxides) [6], as well as various reductive substances (phenols and aromatic amines, etc.) [7]. Although HRP can catalyse the electrochemical reduction of H_2O_2 through a direct electron transfer (DET) mechanism, the electrochemistry of HRP in the absence of H_2O_2, possibly due to its deeply located redox centre and the rather low surface coverage of enzyme on an electrode surface, is rarely observed [8]. Since, for most redox enzymes, DET is a very inefficient process, mediated electrochemical biosensors are typically

Published online: 06 November 2014

used. Mediators can minimise the effects of interferences, lower the operating potential of the electrodes and improve the linear response range and sensitivity of the sensor [9].

Previous literature reports show that direct electrochemistry of HRP has been revealed at carbon nanotubes (CNTs) [10, 11] and metal oxides such as zinc oxide (ZnO) [12], titanium dioxide (TiO_2) [13], mesoporous TiO_2, tin oxide (SnO_2) [14], SnO_2 nanorods [15], SiO_2 nanoparticles [16], nanostructured cerium oxide (CeO_2) [17], nickel oxide nanoparticles (NiO-NPs) [18], polyquaternium–manganese oxide nanosheets [19], zirconia nanocomposites [20] and RuO_2 nanoparticles [21].

Most papers focus on the carbon black [22], glassy carbon [23, 24], gold [25, 26], platinum [27, 28], spectrographic graphite [6, 29], pyrolytic graphite [30, 31] and boron-doped diamond electrodes [32]. However, the high cost and complicated pre-treatment limit their commercial application. Screen-printing technique is a well-established and simple process for mass production of single-use electrodes and biosensors. These electroanalytical tools combine ease of use, portability and inexpensive manufacture procedure [33–35]. The discovery of new nanomaterials opens new paths in the field of sensors. In particular, CNTs have unique properties that have prompted their use in many different applications [36–38].

The adsorption capacity, the possibility to be functionalised, their ability to promote electron transfer reactions of a great number of molecules [39, 40] and the possibility for miniaturisation make CNTs a very attractive material for further development of electrochemical biosensors.

The main aim of the present paper was to study the kinetics of direct and mediated electron transfer of HRP on SPCE, MWCNT-SPCE and SWCNT-SPCE and to see whether a higher percentage of the adsorbed HRP molecules could be in DET contact with the CNT-based electrodes (MWCNT-SPCE and SWCNT-SPCE) than with the graphite based ones (SPCE). The conclusions are based on the comparison of several electrochemical characteristics of HRP on screen-printed carbon electrode (SPCE), screen-printed carbon electrode modified with carboxyl-functionalised multi-wall carbon nanotubes (MWCNT-SPCE) and screen-printed carbon electrode modified with carboxyl-functionalised single-wall carbon nanotubes (SWCNT-SPCE). The second aim of the work was to investigate screen-printed electrodes as basis for construction of biosensors for amperometric determination of H_2O_2 and phenolic compounds using these electrodes with adsorbed HRP.

Experimental

Chemicals

HRP, EC 1. 11.1.7 (268 U mg^{-1} solid), was purchased from Boehringer Mannheim GmbH (Mannheim, Germany). Thirty percent hydrogen peroxide (H_2O_2), catechol, octopamine, 3,4-dihydroxy-L-phenylalanin, pyrogallol, dopamine hydrochloride, ferrocyanide, ferricyanide and salts were from Merck (Darmstadt, Germany). All chemicals were of high purity and used as received. Water purified with a Milli Q system (Millipore, Milford, MA, USA) was used to prepare all solutions.

Biosensor preparation

The SPCE, MWCNT-SPCE and SWCNT-SPCE electrodes were purchased from DropSens (http://www.dropsens.com/, Oviedo, Spain). These screen-printed electrodes include a traditional three-electrode configuration printed on the same strip and have already been described [41]. These screen-printed electrodes present a carbon disk-working electrode with a diameter of 4 mm. The auxiliary electrode (carbon) was printed on each strip using the same ink as the working electrode, and also a printed silver reference electrode. They should be stored at room temperature in a dry place. Eight microliters of the enzyme solution (5 mg mL^{-1}, corresponding to 1,340 U mL^{-1}) was deposited on the surface of the working electrode of SPEs, which were then placed in a petri dish, and adsorption of the enzyme was allowed to proceed overnight at 4 °C. The enzyme electrodes were thoroughly rinsed with 20 mM potassium phosphate buffer, pH 7.0, and if not used immediately they were stored at 4 °C. Weakly adsorbed peroxidase was allowed to desorb before measurements by placing the electrode in a buffer flow for at least 20 min.

Electrochemical experiments

Cyclic voltammetry was performed using a BAS 100 A (USA) with a conventional three-electrode system of SPCE. As electrolyte, 20 mM potassium phosphate buffer at pH 6.0 containing 0.1 M of KCl was used. All voltammetric measurements were carried out at room temperature.

For amperometric studies at constant applied potential in the flow mode, the enzyme electrodes were placed into a methacrylate wall-jet flow electrochemical cell (DropSens). Due to the transparency of the material, any possible presence of bubbles is easily detectable. The enzyme electrode was connected using a cable connector to a potentiostat (Zeta Elektronik, Höör, Sweden) and the current was recorded. The measurements were performed at an applied potential of 0 mV versus printed silver. The flow cell was connected to a flow-injection system consisting of peristaltic pump (Gilson Minipuls 3, Villier-le-Bel, France) and an electrical six-port valve injector (Rheodyne; RTP Company, Cotati, CA, USA) supplied with a 50-μL injection loop and carefully calibrated. Through the flow system, a 20 mM potassium phosphate buffer at pH 6.0 was used as the flow carrier. H_2O_2 of various concentrations, always freshly prepared, was either injected

into the flow buffer for FIA measurements or supplied in the flow buffer for steady-state measurements. The solutions were degassed before use to prevent microbubbles to appear in the system. All experiments were performed at room temperature.

Results and discussion

Electrochemical behaviour of screen-printed electrodes

Cyclic voltammograms (CVs) of ferro/ferricyanide using the three different screen-printed carbon electrodes are shown in Fig. 1. As can be easily seen, the electrochemistry described by a well-defined pair of redox peaks characteristic of the ferri/ferrocyanide redox couple occurred on the naked screen-printed electrodes. The formal potential determined as the midpoint of the anodic and cathodic peak versus printed silver is about 143.5, 120.5 and 129.5 mV for SPCE, MWCNT and SWCNT, respectively. Moreover, the peak-to-peak separation ΔEp was found to be 215 and 155 mV for SPCE and MWCNT at a scan rate of 25 mV s^{-1}, whereas the one for SWCNT is close to 97 mV and the ratio of redox peak current Ipa/Ipc was 1.00, suggesting the occurrence of a quasi-reversible redox reaction at the surface of screen-printed electrodes. What is also clear from the CVs shown in Fig. 1 is that the ferri/ferrocyanide electrochemistry on SWCNT-SPCE and MWCNT-SPCE was facilitated due to a large nanostructured surface area, π-conjugated systems of sp^2-carbon atoms and large amounts of conductive sites available on the surface of electrode.

Catalytic activity screen-printed electrodes towards to H_2O_2

In Fig. 2a–c are shown CVs of HRP-modified SPCE (Fig. 2a), MWCNT-SPCE (Fig. 2b) and SWCNT-SPCE (Fig. 2c) in pure buffer and in buffer also containing 4 mM H_2O_2. As is clear from these figures, no voltammetric waves were

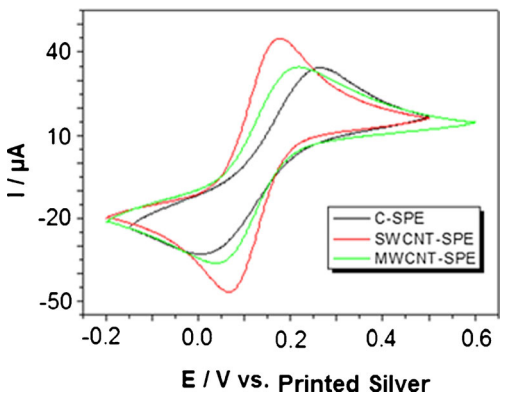

Fig. 1 Cyclic voltammograms of 2.5 mM $Fe(CN)_6^{4-/3-}$ for the different types of SPE in 20 mM phosphate buffer, pH 6 containing 0.1 M KCl

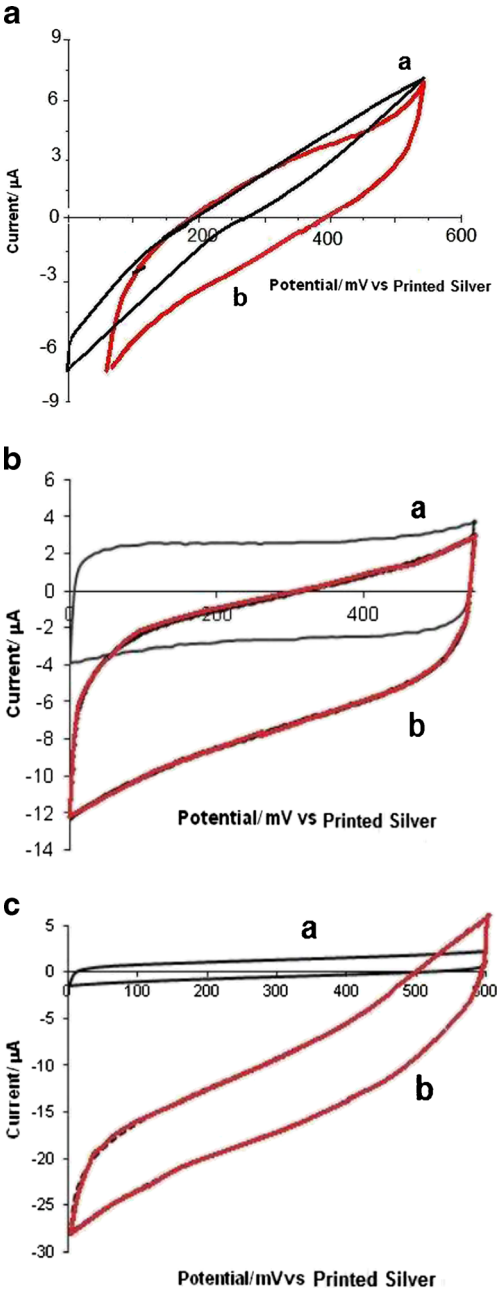

Fig. 2 Cyclic voltammograms of the HRP-modified screen-printed carbon electrode in 20 mM phosphate buffer, pH 6, scan rate 50 mV s^{-1}, **a** plain buffer and **b** 4 mM H_2O_2. **A** HRP-modified SPCE. **B** HRP-modified MWCNT-SPCE. **C** HRP-modified SWCNT-SPCE

observed for any of the HRP-modified electrodes in pure buffer. The cyclic voltammograms displayed low background current for HRP-modified SWCNT-SPCE comparatively to HRP-modified SPCE and HRP-modified MWCNT-SPCE. However, when 4 mM H_2O_2 is added to the buffer, the voltammograms show a high reduction current, which corresponds to an electron transfer leading to the reduction of hydrogen peroxide by the presence of HRP acting as an efficient electrocatalyst. Too low increase in current was observed if H_2O_2 was added when using HRP-modified screen-

printed electrode (Fig. 2a). These results clearly illustrate that DET occurred on screen-printed electrodes in the presence of HRP.

In addition, one can observe that the catalytic current corresponding to hydrogen peroxide reduction at the HRP-immobilised screen-printed electrodes starts at +600 mV versus printed silver confirming that the reaction occurs through the peroxidase cycle with the formation of compound I and II [1–5]. It is also clear that the electrocatalytic efficiency for reduction of H_2O_2 on SWCNT-HRP (Fig. 2c) is much higher leading to a higher reduction current than on MWCNT-HRP (Fig. 2b) and also on SPCE (Fig. 2a). This result demonstrates that SWCNT displays a large and effective surface facilitating a fast electron transfer.

Optimisation of the experimental conditions for amperometry in the flow mode

The influence of the flow rate applied to the wall-jet flow electrical cell was studied by measurement of the peak currents for H_2O_2 using the HRP-modified SPCE, MWCNT-SPCE and SWCNT-SPCE (not shown). The results showed that the highest current peaks were obtained at low flow rates due to kinetic restrictions at the HRP-modified surface even though a higher flow rate leads to a more efficient mass transfer of the H_2O_2 to the electrode surface. Also, the results showed that the response currents are much higher on the HRP-modified SWCNT-SPCE and MWCNT-SPCE than on the HRP-modified SPCE. For comparison of electrochemical behaviour of electrodes, a flow rate of 0.225 mL min^{-1} was chosen for experiments as the highest currents were obtained at this flow rate.

The maximum response current to H_2O_2 at the HRP-modified electrodes depends on the pH of the buffer solution, which governs the activity of the enzyme and also the efficiency of the reduction of the oxidised form of HRP by the electrode. The effect of pH value on the catalytic activity of the HRP-modified screen-printed electrodes was studied. It was found that all the three investigated screen-printed HRP-modified electrodes exhibited the highest catalytic activity in pH 6.0 (not shown). This value was chosen for the subsequent determinations. To optimise the amount of immobilised enzyme, different amounts of HRP were tested by modification of the SPCE, MWCNT-SPCE and SWCNT-SPCE. The maximum signal was obtained for 0.04 mg of HRP (Fig. 3). Therefore, it was used for further experiments.

Kinetic model of peroxidase action on SPCE, MWCNT-SPCE and SWCNT-SPCE

The basic reaction of HRP includes its oxidation by hydrogen peroxide (H_2O_2) and then subsequent reduction of the enzyme

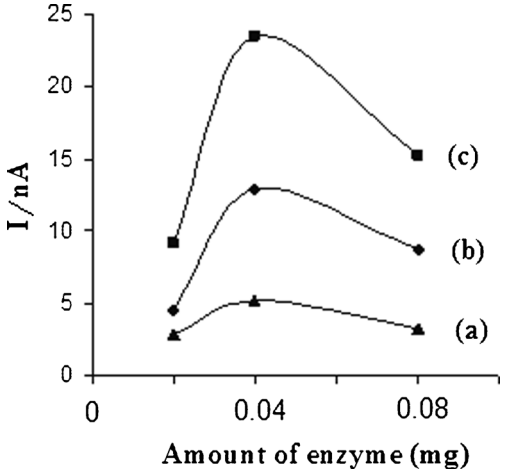

Fig. 3 Response currents obtained for **a** SPCE, **b** MWCNT-SPCE and **c** SWCNT-SPCE for injections of 50 μM H_2O_2 in 20 mM phosphate buffer, pH 6.0. Applied potential 0 V versus printed silver at 0.225 mL min^{-1} flow rate

by electrons provided by an electron donor according to reactions (2) and (3):

$$HRP + H_2O_2 \rightarrow Cpd\ I + H_2O \quad (k_1) \tag{1}$$

$$Cpd\ I + AH_2 \rightarrow Cpd\ II + AH\bullet \quad (k_2) \tag{2}$$

$$Cpd\ II + AH_2 \rightarrow HRP + AH\bullet + H_2O \quad (k_3) \tag{3}$$

Where HRP is the native ferric enzyme, Cpd I and Cpd II are oxidised intermediates, compound I and II, respectively, and AH_2 and AH• are the electron donor substrate and the radical product of its one-electron donor oxidation. The enzyme immobilised on an electrode surface can be oxidised by H_2O_2 according to reaction (1) and then subsequently reduced by electrons provided by an electrode, reaction (4):

$$Cpd\ I + 2e^- + 2H^+ \rightarrow HRP + H_2O \quad (k_s). \tag{4}$$

This process is usually referred to as DET, i.e. when an electrode substitutes the electron donor substrates in a common peroxidase cycle, reactions (1)–(3). When an electron donor is present in a peroxidase–electrode system, both processes can occur simultaneously and the oxidised donor AH• is electrochemically reduced by an electrode according to reaction (5):

$$AH\bullet + e^- + H^+ \rightarrow AH_2 \quad (k_s) \tag{5}$$

When the reaction cycle goes through reactions (1) to (3) and followed by reaction (5), the electron transfer is denoted

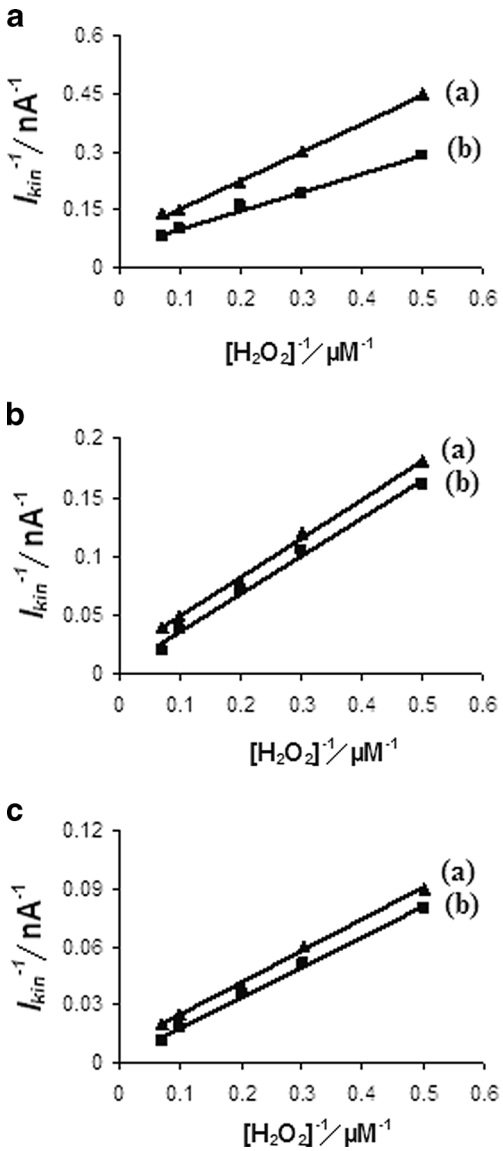

Fig. 4 Plot of the inverted kinetically limited currents (I_{kin}^{-1}, obtained as intercepts of Koutecky–Levich plots) versus $[H_2O_2]^{-1}$ for **A** HRP-modified SPCE, **B** HRP-modified MWCNT-SPCE and **C** HRP-modified SWCNT-SPCE in **a** the absence and **b** the presence of 50 μM catechol

mediated electron transfer (MET), which is known to be more efficient compared with direct ET [42].

To compare the electrochemical properties of HRP on the various electrodes, the kinetic constants for direct and mediated ET were calculated from wall-jet flow electrical cell experiments. The reduction current for H_2O_2 at HRP-modified electrodes can be limited by the mass transfer of H_2O_2 to the electrode or by the kinetics of the enzymatic reaction. The measured current, I, is described by the following equation:

$$1/I = 1/I_{\text{lim}} + 1/I_{\text{kin}} \quad (6)$$

where I_{lim} is the mass-transfer limited current and I_{kin} is the kinetically limited current. Varying the flow rate or varying the concentration of the substrate in the solution can change the mass-transfer current for a wall-jet system. The kinetically limited current due to direct electron transfer can be expressed as [6]:

$$1/I_{\text{kin}} = 1/nFE_{\text{DET}}(1/k_1c^* + 1/k_s) \quad (7)$$

where n is the number of electrons transferred per H_2O_2 molecule (n=2), c* is the bulk concentration of H_2O_2, E_{DET} is the amount of enzyme active in DET contact and F is the Faraday constant. By fitting the dependence of I_{kin} against the H_2O_2 concentration according to Eq. (7), the kinetic constants k_1 and k_s can be evaluated (see Fig. 4).

In the presence of saturating concentrations of a donor substrate, all peroxidase molecules work in MET [29]. Thus, the kinetically limited current is expressed as follows:

$$1/I_{\text{kin}} = 1/2nFE(1/k_1c^* + 1/k_3[\text{AH}_2]) \quad (8)$$

where n is the number of electrons transferred per donor molecule (n=1), E is the total amount of active enzyme on the electrode surface and k_3 is the rate-limiting constant for the enzyme reduction by the substrate AH_2. By fitting the dependence of I_{kin} against the H_2O_2 concentration according to Eq. (8), the kinetic constants k_1 and k_3 can be evaluated (see Fig. 4).

The slope of these plots, obtained in the presence and in the absence of an electron donor (in this case catechol), is the ratio between the enzyme active in DET and the total amount of active enzyme [6]. This ratio and the kinetic constants of HRP at the surface of the three types of investigated electrodes are presented in Table 1. Although the absolute values of the rate

Table 1 The percentage of active peroxidase molecules in direct ET and the electrochemically determined rate constants for HRP adsorbed on screen-printed electrodes (number of tested electrodes, n=3)

Electrode	% in direct ET	k_1 (10^5 M^{-1} s^{-1})	k_s (s^{-1})	k_3 (10^4 M^{-1} s^{-1})
SWCNT-SPCE	105±2	0.49±0.05	1.2±0.1	3.3±0.1
MWCNT-S	100±2	0.23±0.03	1.0±0.06	1.5±0.1
SPCE	65±5	0.10±0.01	0.60±0.07	1.3±0.2

50 μM catechol was used for the determination of k_3

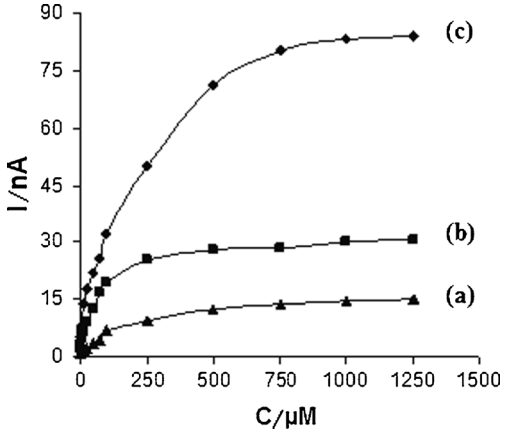

Fig. 5 Calibration curves for H_2O_2 obtained using the wall-jet system for **a** HRP-modified SPCE, **b** HRP-modified MWCNT-SPCE and **c** HRP-modified SWCNT-SPCE electrodes

constants obtained from electrochemical kinetics are not very precise (since the true surface concentration of HRP remains unknown), this method can be used with precaution to compare the efficiency of HRP on the different electrodes. As shown in Table 1, the ET reaction between HRP and SPCE (k_1) was lower than those between HRP and MWCNT-SPCE or SWCNT-SPCE. Differences in the apparent efficiency of ET is related to the large specific surface area, large amounts of conductive sites, large surface roughness of carbon nanotubes and to the differences in the surface states of the carbon materials used in electrodes, changing from π-conjugated systems of sp^2-carbon atoms characteristic for carbon nanotubes to the surface sp^3-carbon states of carbon. These new electrodes offer better electron transfer than most conventional screen-printed electrodes, while retaining the electrocatalytic properties of the nanotubes. In quantity, it is expected that there are more enzyme molecules immobilised on the surface of SWCNT-SPCE followed by MWCNT-SPCE compared with SPCE. This would yield a higher response current. However, obviously there is also a great influence through that on the SWCNT- and MWCNT-modified screen-printed electrodes a much higher percentage of the adsorbed HRP molecules that are directed to DET (around 100 %) compared with only around 65 % on the graphite-based electrodes, which is in accordance with previous results on graphite [6, 29].

Determination of hydrogen peroxide

The peroxidase electrodes were used to determine hydrogen peroxide in mediatorless WJE mode. H_2O_2 was added in small portions to the flow buffer, and the steady-state current was recorded after each addition. Representative calibration curves are presented for SPCE, MWCNT-SPCE and SWCNT-SPCE in Fig. 5 exhibiting typical Michaelis–Menten behaviour. The detection limits for the various electrodes were calculated from the calibration curves (signal-to-noise ratio of 3) and are presented in Table 2. As seen, SWCNT-SPCE gave the lowest detection limit (0.40±0.09 μM). MWCNT-SPCE gave only a slightly higher detection limit (0.48±0.07 μM), whereas SPCE gave an even higher detection limit (0.98±0.2 μM). The sensitivities of the sensors were calculated from the initial slope of the calibration curves. SWCNT-SPCE shows the highest sensitivity (5.1±0.2 nA μM^{-1} cm^{-2}), slightly higher than the sensitivity of MWCNT-SPCE (4.5±0.3 nA μM^{-1} cm^{-2}) and almost three times as high as the one calculated for SPCE (1.6±0.1 nA μM^{-1} cm^{-2}). Additional characteristics such as apparent Michaelis–Menten constant (K_M^{app}) was obtained by direct fitting of the calibration data to the Michaelis–Menten equation ($I = cI_{max}$ ($c + K_M^{app}$)). As can be observed, SPCE biosensors modified with carbon nanotubes (SWCNT-SPCE and MWCNT-SPCE) exhibited excellent performance in terms of low detection limit, low value of K_M^{app} and high sensitivity because of the large surface area and porous nature of the CNT-modified surfaces

Table 2 Comparison of the performance of the hydrogen peroxide biosensors based on HRP

Electrode	LR (μM)	LOD (μM)	(S) (nA μM^{-1} cm^{-2})	K_M^{app} (μM)	Reference
HRP-Nafion-sonogel-carbon	4–100	1.60	12.8	295	[43]
HRP-GSH/Au	1–120	0.40	–	3,120	[44]
HRP/TMB/AuS/ITO	5–1,500	1.00	–	2,200	[45]
HRP-SiO_2-MB-gelation-GC	10–1,200	0.40	–	900	[46]
HRP/organosilica@chitosan/MWNTs/GCE	0.7–2,800	0.25	49.8	320	[47]
HRP-SPCE	5.98–35.36	–	0.14	–	[48]
SWCNT-SPCE	0.5–500	0.40±0.09	5.1±0.2	7.6±0.3	This work
MWCNT-SPCE	0.5–250	0.48±0.07	4.5±0.3	8.6±0.4	This work
SPCE	1–250	0.98±0.2	1.6±0.1	16±0.8	This work

Number (n) of tested electrodes in this work is 3

GSH L-glutathione, *TMB* tetramethyl benzidine, *ITO* indium–tin oxide electrode, *MB* methylene blue, *GC* glassy carbon, *LR* linear range, *LOD* limit of detection, *S* sensitivity, k_M^{app} Michaelis–Menten constant

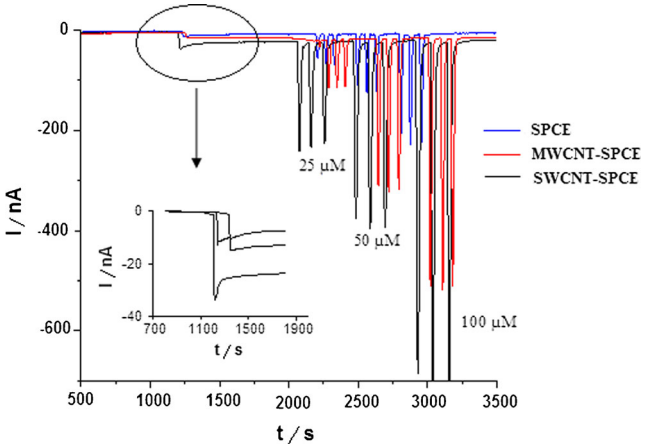

Fig. 6 Steady-state current for 50 µM H_2O_2 in flow buffer and flow-injection peaks for catechol registered for the different HRP-modified screen-printed electrodes. The *inset* shows steady-state currents for the electrodes

assisting both in the entrapment of more HRP as well as in a higher percentage of enzyme molecules in DET contact with the electrode. Also, the analytical performance of HRP-modified SPCEs developed in this study was compared with other HRP-based hydrogen peroxide biosensors previously reported in the literature [43–48]; see Table 2.

The fabrication reproducibility of three modified electrodes, made independently, showed an acceptable reproducibility for the current determination of 0.01 mM hydrogen peroxide with the relative standard deviations of 4.2, 3.5 and 3.8 % for SWCNT-SPCE, MWCNT-SPCE and SPCE, respectively.

Amperometric detection of phenols

The enzyme intermediates, compound I and compound II, can be reduced back electrochemically in two ways, by either through DET or MET reaction pathways [7]. If the peroxidase-modified electrodes are used as sensors in a flow system, a continuous supply of H_2O_2 in the carrier results in a steady-state current due to the direct electrochemical reduction of adsorbed HRP molecules. If a sample containing a donor substrate such as phenols [49, 50], aromatic amines [51, 52] is injected, the peroxidase molecules both those directed for DET as well as those only available for MET will be switched on and electrochemical response peaks can be observed on top of the steady-state current (see Fig. 6), and the reduction peak currents will be proportional to the concentration of the donor. At optimal conditions, different phenolic compounds have been tested using peroxidase-modified electrodes. As can be seen (Fig. 6, inset), the HRP-modified SWCNT-SPCE followed by the HRP-modified MWCNT-SPCE showed both high steady-state currents for H_2O_2 and high flow-injection response peaks for catechol. The corresponding currents registered for HRP-modified SPCE are substantially lower. These results show that obviously much higher surface concentrations of HRP on the SWCNT-SPCE and MWCNT-SPCE are possible in combination with higher reaction rates (see Table 1) than on the corresponding SPCE. The sensitivities and detection limits obtained for a number of phenolic compounds are presented in Table 3, from which one can see that HRP on SPCE, MWCNT-SPCE and SWCNT-SPCE differs in their sensitivities and, thus, in activities toward various phenolic compounds. The phenolic compounds have the lowest detection limit on SWCNT-SPCE followed by MWCNT-SPCE, probably due to the large amounts of conductive sites available on the surface for contacting with enzyme molecules. The sensitivity of phenolic compounds at MWCNT-SPCE and SWCNT-SPCE was improved in comparison to the response observed at SPCE. Differences in the sensitivity are related to the large specific surface area of carbon nanotubes.

Interference study

In real samples, some co-existing electroactive species might affect the biosensor response, for example, uric acid, cysteine, glutathione, tryptophan, tyrosine and methionine. The selectivity and anti-interference advantages are demonstrated by comparing the responses of relevant electroactive species (0.01 mM) on a modified electrode. The results showed that mentioned compounds do not have interference to detection of H_2O_2. The good ability of anti-interference was largely

Table 3 Detection limits (LOD, calculated as three times the noise) and sensitivities (S) for phenolic compounds from calibration data using different electrodes (n=2)

Substance	SWCNT-SPCE		MWCNT-SPCE		SPCE	
	LOD (nM)	S (nA µM^{-1} cm^{-2})	LOD (nM)	S (nA µM^{-1} cm^{-2})	LOD (nM)	S (nA µM^{-1} cm^{-2})
Catechol	110.2±3.6	83.60±4.2	280.1±7.8	33.20±1.1	720.4±12	25.53±0.61
Dopamine	640.2±9.2	30.40±5.1	770.8±11	22.30±0.45	4,341±25	2.072±0.24
Octopamine	3,341±15	2.102±0.31	3,201±17	2.151±0.13	5,071±15	1.283±0.30
Pyrogallol	50.10±2.9	448.2±9.5	90.90±3.2	242.4±7.2	130/4±8.6	189.3±9.2
L-Dopa	980.7±8.7	9.204±0.42	4,503±22	4.501±0.24	4,901±13	1.224±0.42

attributed to the low working potential used in the determination of H_2O_2.

Conclusion

This manuscript is based on the comparison of several direct and mediated electrochemical characteristics of HRP on SPE, MWCNT-SPCE and SWCNT-SPCE in optimal conditions. It is demonstrated that the signal response on SWCNT-SPCE followed by MWCNT-SPCE is increased in comparison with SPCE. The screen-printed carbon electrodes modified with carboxyl-functionalised carbon nanotubes facilitate DET between the active site of HRP and electrodes due to a large nanostructured surface area and large amounts of conductive sites available on the surface establishing contact with the enzyme molecules with retained electrocatalytic properties of the nanotubes. This is shown through a higher percentage in DET contact with the electrode. In addition, the enzyme has superior electrochemical characteristics on carbon nanotubes modified screen-printed electrodes reflected by higher rate constants, allowing highly sensitive determination of hydrogen peroxide and phenolic compounds. The data obtained in this study is summarised in Tables 1, 2 and 3.

References

1. Ruzgas T, Gorton L, Emnéus J, Marko Varga G (1995) J Electroanal Chem 391:41–49
2. Veitch NC (2004) Phytochemistry 65:249–259
3. Dzyadevych SV, Arkhypova VN, Soldatkin AP, Elskaya AV, Martelet C, Jaffrezic-Renault N (2008) ITBM-RBM 29:171–180
4. Habermüller K, Mosbach M, Schuhmann W (2000) J Anal Chem 366:560–568
5. Battistuzzi G, Stampler J, Bellei M et al (2011) Biochemistry 50: 7987–7994
6. Lindgren A, Ruzgas T, Gorton L, Csoregi E, Ardila GB, Sakharov IY, Gazaryan IG (2000) Biosens Bioelectron 15:491–497
7. Lindgren A, Emneus J, Ruzgas T, Gorton L, Marko-Varga G (1997) Anal Chim Acta 347:51–62
8. Konash A, Magner E (2006) Biosens Bioelectron 22:116–123
9. Periasamy AP, Yang S, Chen SM (2011) Talanta 87:15–23
10. Yang Y, Yang G, Huang Y, Bai H, Lu X (2009) Colloids Surf A 340: 50–55
11. Wang S, Xie F, Liu G (2009) Talanta 77:1343–1350
12. Xiang C, Zou Y, Sun LX, Xu F (2009) Sens Actuators B 136:158–162
13. Wang Y, Ma X, Wen Y, Xing Y, Zhang Z, Yang H (2010) Biosens Bioelectron 25:2442–2446
14. Astuti Y, Topoglidis E, Cass AG, Durrant JR (2009) Anal Chim Acta 648:2–6
15. Liu J, Li Y, Huang X, Zhu Z (2010) Nanoscale Res Lett 5:1177–1181
16. He P, Hu N (2004) Electroanalysis 16:1122–1131
17. Ansari AA, Solanki PR, Malhotra BD (2009) J Biotechnol 142:179–184
18. Mohammadi A, Moghaddam AB, Kazemzad M, Dinarvand R, Badraghi J (2009) Mater Sci Eng C 29:1752–1758
19. Yang X, Chen X, Zhang X, Yang W, Evans DG (2008) Sens Actuators B 134:182–188
20. Zong S, Cao Y, Zhou Y, Ju H (2006) Langmuir 22:8915–8919
21. Periasamy AP, Ting SW, Chen SM (2011) Int J Electrochem Sci 6: 2688–2709
22. Yaropolov AI, Tarasevich MR, Vorfolomeev SD (1978) Bioelectrochem Bioenerg 5:18–24
23. Kong YT, Boopathi M, Shim YB (2003) Biosens Bioelectron 19: 227–232
24. Jiangwen L, Lihong L, Fei X, Hhe G, Rui Y, Faqiong Z, Ling H, Baizhao Z (2008) J Electroanal Chem 613:51–57
25. Song Y, Wang L, Ren C, Zhu G, Li Z (2006) Sens Actuat B 114: 1001–1006
26. Zhongqiang T, Ruo Y, Yaqin C, Shihong C, Yi X (2007) Biotechnol Lett 29:791–795
27. Adeyoju O, Iwuoha EI, Smyth MR (1994) Anal Proc 31:177–179
28. Comtat M, Durliat H (1994) Biosens Bioelectron 9:663–668
29. Lindgren A, Munteanu FD, Gazayan IG, Ruzgas T, Gorton L (1998) J Electroanal Chem 458:113–120
30. Huang R, Hu N (2001) Bioelectrochemistry 54:75–81
31. Tarasevich MR, Bogdanovskaya VA, Fridman VA, Kuznetsova LN (2001) Russ J Electrochem 37:730–734
32. Tatsuma T, Mori H, Fujishima A (2000) Anal Chem 72:2919–2924
33. Hart JP, Wring SA (1994) Electroanalysis 6:617–624
34. Hart JP, Wring SA (1997) Trends Anal Chem 16:89–103
35. Honeychurch KC, Hart JP (2003) Trends Anal Chem 22:456–469
36. Merkoci A, Pumera M, Llopis X, Perez B, Del Valle M, Alegret S (2005) Trends Anal Chem 24:826–838
37. Wang J, Liu G, Jan MR (2004) J Am Chem Soc 126:3010–3011
38. Robertson J (2004) Mater Today 7:46–52
39. Luo H, Shi Z, Li N, Gu Z, Zhuang Q (2001) Anal Chem 73:915–920
40. Musameh M, Wang J, Merkoc i A, Lin Y (2002) Electrochem Commun 4:743–746
41. García-González R, Fernández-Abedul MT, Pernía A, Costa-García A (2008) Electrochim Acta 53:3242–3249
42. Lindgren A, Tanaka M, Ruzgas T, Gorton L, Gazaryan I, Ishimori K, Morishima I (1999) Electrochem Commun 1:171–175
43. Elkaoutit M, Naranio-Rodrigueza I, Domínguez M, Hernandez-Artig MP, Bellido-Milla D, De Cisnerosa JLHH (2008) Electrochim Acta 53:7131–7137
44. Liu CY, Hu JM (2008) Chin Chem Lett 19:955–958
45. Lin J, Zhang L, Zhang S (2007) Anal Biochem 370:180–185
46. Yao H, Li N, Xu S, Xu JZ, Zhu JJ, Chen HY (2005) Biosens Bioelectron 21:372–377
47. Chen S, Yuan R, Chai Y, Yin B, Li W, Min L (2009) Electrochim Acta 54:3039–3046
48. Teng YJ, Zuo SH, Lan MB (2009) Biosens Bioelectron 24:1353–1357
49. Rosatto SS, Sotomayor PT, Kubota LT, Gushikem Y (2002) Electrochim Acta 47:4451–4458
50. Santos AS, Pereira AC, Sotomayor MDPT, Tarley CRT, Durán N, Kubota LT (2007) Electroanalysis 19:549–554
51. Munteanu FD, Lindgren A, Emnéus J, Gorton L, Ruzgas T, Csöregi E, Ciucu A, Huystee RBV, Gazaryan IG, Lagrimini LM (1998) Anal Chem 70:2596–2600
52. Li J, Xiao LT, Liu XM, Zeng GM, Huang GH, Shen GL, Yu RQ (2003) Anal Bioanal Chem 376:902–907